Period bouncers as detached magnetic cataclysmic variables

Schreiber, M.R.; Belloni, D.; van Roestel, J.

DOI
10.1051/0004-6361/202347766
Publication date
2023
Document Version
Final published version
Published in
Astronomy & Astrophysics

A&A 679, L8 (2023)
https://doi.org/10.1051/0004-6361/202347766

Astronomy & Astrophysics

LETTER TO THE EDITOR

Period bouncers as detached magnetic cataclysmic variables

Matthias R. Schreiber[1,2], Diogo Belloni[1], and Jan van Roestel[3]

[1] Departamento de Física, Universidad Técnica Federico Santa María, Av. España 1680, Valparaíso, Chile
e-mail: matthias.schreiber@usm.cl; diogobellonizorzi@gmail.com
[2] Millennium Nucleus for Planet Formation, Valparaíso, Chile
[3] Anton Pannekoek Institute for Astronomy, University of Amsterdam, 1090 GE Amsterdam, The Netherlands

Received 20 August 2023 / Accepted 6 October 2023

ABSTRACT

Context. The general prediction that more than half of all cataclysmic variables (CVs) have evolved past the period minimum is in strong disagreement with observational surveys, which show that the relative number of these objects is just a few percent.
Aims. Here, we investigate whether a large number of post-period minimum CVs could detach because of the appearance of a strong white dwarf magnetic field potentially generated by a rotation- and crystallization-driven dynamo.
Methods. We used the MESA code to calculate evolutionary tracks of CVs incorporating the spin evolution and cooling as well as compressional heating of the white dwarf. If the conditions for the dynamo were met, we assumed that the emerging magnetic field of the white dwarf connects to that of the companion star and incorporated the corresponding synchronization torque, which transfers spin angular momentum to the orbit.
Results. We find that for CVs with donor masses exceeding ∼0.04 $M_{\odot}$, magnetic fields are generated mostly if the white dwarfs start to crystallize before the onset of mass transfer. It is possible that a few white dwarf magnetic fields are generated in the period gap. For the remaining CVs, the conditions for the dynamo to work are met beyond the period minimum, when the accretion rate decreased significantly. Synchronization torques cause these systems to detach for several gigayears even if the magnetic field strength of the white dwarf is just one MG.
Conclusions. If the rotation- and crystallization-driven dynamo – which is currently the only mechanism that can explain several observational facts related to magnetism in CVs and their progenitors – or a similar temperature-dependent mechanism is responsible for the generation of magnetic field in white dwarfs, most CVs that have evolved beyond the period minimum must detach for several gigayears at some point. This reduces the predicted number of semi-detached period bouncers by up to ∼60−80%.

Key words. binaries: close – stars: magnetic field – methods: numerical – white dwarfs

1. Introduction

According to the standard theory for the formation and evolution of cataclysmic variables (CVs, Belloni & Schreiber 2023; Knigge et al. 2011), and independent of the details of simulating CV evolution, a large number of all CVs should already have passed the period minimum, that is, the population of CVs should be dominated by systems evolving toward longer orbital periods consisting of a cool white dwarf with a brown dwarf companion. The predicted fraction of these so-called period bouncers among CVs was estimated decades ago to be 70% (Kolb 1993), a value roughly in agreement with more recent calculations, which predict 38−60% (Goliasch & Nelson 2015) and ∼75% (Belloni et al. 2018).

However, despite significant observational efforts, very few period bouncers have so far been identified. Patterson (2011) heard some murmurs from the period bounce by identifying 22 candidates among the CVs known at that time. More recently, Pala et al. (2020) found the fraction of period bouncers to be 7−14% in a volume-limited sample of CVs. Dedicated surveys for CVs in the data releases of the Sloan Digital Sky Survey (SDSS) confirm that the fraction of period bouncers does not exceed a few percent (Inight et al. 2023a,b). This large discrepancy between theoretical prediction and observations might be the most important problem in our understanding of CV evolution.

A potentially important ingredient in CV evolution – that was ignored in binary population models of CVs for decades – is the possible impact of white dwarf magnetic fields, despite the fact that more than one-third of all CVs in volume-limited samples host a magnetic white dwarf (Pala et al. 2020). Observations of both single white dwarfs (Bagnulo & Landstreet 2021) and detached white dwarf binaries with M-dwarf companions (Parsons et al. 2021) clearly show that the vast majority of white dwarf magnetic fields appear when the white dwarf has significantly cooled, that is, either the magnetic field is buried for several gigayears (Gyr) after the white dwarf formation, or the conditions for generating a magnetic field are met only in cool white dwarfs.

Based on these observational facts and the early work by Isern et al. (2017), we developed the idea of a rotation- and crystallization-driven magnetic dynamo that generates strong white dwarf magnetic fields during CV evolution (Schreiber et al. 2021). According to this model, white dwarfs that crystallize before mass-transfer starts generate a strong magnetic field as soon as accretion has spun up the white dwarf. If the emerging magnetic field connects with that of the donor star, spin angular momentum is transferred to the orbit, which causes

the separation of both stars to increase and the CV to convert into a detached binary. Loss of angular momentum through gravitational radiation and/or reduced magnetic braking (Belloni et al. 2020) then slowly shrinks the orbit until the donor fills its Roche lobe and the system becomes a magnetic CV.

While the assumption of magnetic field generation through the dynamo is rather speculative (as other ideas for the origin of magnetic fields in white dwarfs are), the described evolutionary scenario can reproduce a number of observations that otherwise remain inexplicable: (i) the fact that so far all observed detached close binaries containing a strongly magnetic white dwarf are close to Roche-lobe filling and typically have periods of between 3 and 5 h; (ii) the existence of the radio pulsing white dwarf binaries AR Sco (Marsh et al. 2016) and eRASSU J191213.9–441044 (Pelisoli et al. 2023); (iii) the small number of high-accretion-rate magnetic CVs in globular clusters (Belloni et al. 2021); and (iv) the observed magnetic fields in detached double white dwarfs (Schreiber et al. 2022).

Here we focus on magnetic field generation and angular momentum transfer for systems that evolve toward and beyond the period minimum as nonmagnetic CVs. In these systems, the mass-transfer rate becomes small enough to allow the core of the white dwarf to crystallize, and according to the dynamo idea, the white dwarf should develop a magnetic field. The corresponding synchronization torques should then cause the system to detach for several Gyr, thereby reducing the number of predicted period bouncers significantly.

2. The model

We used the MESA code (Paxton et al. 2011, 2013, 2015, 2018, 2019; Jermyn et al. 2023, r15140) to compute the evolution of CVs as in Schreiber et al. (2021). The initial conditions for all our simulations are detached post-CE binaries with different initial donor star and white dwarf masses and orbital periods.

We assumed angular momentum loss through magnetic braking according to Rappaport et al. (1983) and through gravitational radiation, and that magnetic braking gets disrupted when the donor star becomes fully convective. We used normalization factors to calibrate the strength of angular momentum loss. We also considered the empirical prescription for consequential angular momentum loss found by Schreiber et al. (2016), which is required to bring the observed and predicted white dwarf mass distributions into agreement.

Angular momentum accretion and spin-up of the white dwarf during mass transfer was calculated as in Schreiber et al. (2021), that is, largely following King et al. (1991). The potential connection between the emerging white dwarf magnetic field and that of the donor star, as well as the resulting angular momentum transfer of spin angular momentum to orbital angular momentum, were also treated as in Schreiber et al. (2021).

In line with Ginzburg et al. (2022), we assumed the critical spin period to be one hour, which is significantly longer than the values assumed by Schreiber et al. (2021). We also updated our model by incorporating a diffusion timescale that reflects the time the field requires to reach the surface of the white dwarf after the conditions for magnetic field generation are met in the core (Ginzburg et al. 2022).

Crystallization depends on the core temperature of the white dwarf, which is therefore of fundamental importance for magnetic field generation in our model. We assumed the critical temperature for the dynamo to work to be the temperature corresponding to the onset of crystallization, as provided by the thick hydrogen atmosphere models of Bédard et al. (2020). The core temperature of cooling single white dwarfs can be reliably determined from these evolutionary sequences.

The most important update compared to our previous modeling of CV evolution including magnetic field generation through the rotation- and crystallization-driven dynamo concerns the heating of the white dwarf core through accretion. Accretion can slowly (on a timescale of a few 100 million years) heat up the core until an equilibrium at the base of the radiative layer is reached.

Incorporating the full details of cooling and heating of accreting white dwarfs in our simulations is beyond the scope of this Letter. However, based on published results (Townsley & Bildsten 2004; Epelstain et al. 2007; Townsley & Gänsicke 2009), we developed a simple prescription that should cover the main physics. Briefly, we used the cooling temperature for nonaccreting white dwarfs while for accreting white dwarfs we slowly increased the core temperature until the equilibrium core temperature (governed by the mass accretion rate) was reached.

We are aware that our modeling approach is based on several assumptions, such as the stellar field strengths, the accretion efficiency of angular momentum, and the synchronization or diffusion timescales. In addition, our prescription for determining the white dwarf core temperature during accretion is clearly a simplified representation of reality. However, the general idea of the scenario is independent of the exact values and procedures that we assumed in our modeling. More details can be found in Schreiber et al. (2021) and Appendix A. The code we used to calculate the evolutionary tracks can be found online[1].

3. Evolutionary pathways

Figure 1 shows two evolutionary tracks for CVs that start mass transfer above the orbital period gap, together with observed period bouncers and the detached magnetic white dwarf with a brown dwarf companion SMSSJ 160639.78−100010.7 (see Appendix B for more details on the observed systems). The red dashed lines represent a case similar to those described in Schreiber et al. (2021), that is, mass transfer starts when the white dwarf core has already started to crystallize. The magnetic field is generated in the core of the white dwarf when the critical rotation rate is reached. The field then diffuses outward and when it emerges at the surface, it can connect with the field of the secondary star and synchronization torques lead to the transfer of spin angular momentum to the orbit, and the binary becomes a detached system. The model predicts the detached binary to first resemble AR Sco (Marsh et al. 2016) and later, when spin and orbit are synchronized, to become a pre-polar (Parsons et al. 2021).

The black solid line corresponds to the case of a white dwarf that is still far from crystallizing when mass transfer starts. This prevents the system from generating a magnetic field above the gap because accretion keeps the core temperature above the crystallization limit. The system detaches at the upper edge of the orbital period gap as predicted by standard CV evolution theory. While crossing the gap, the white dwarf cools but not enough to start crystallizing because with residual magnetic braking, the evolution through the gap takes only ∼300 Myr. When mass transfer resumes below the gap, accretion determines the core temperature. As the mass-accretion rate decreases significantly when the donor converts into a brown dwarf and the system passes the orbital period minimum, the core temperature of the white dwarf inevitably reaches the crystallization limit at some

[1] https://zenodo.org/records/10008722

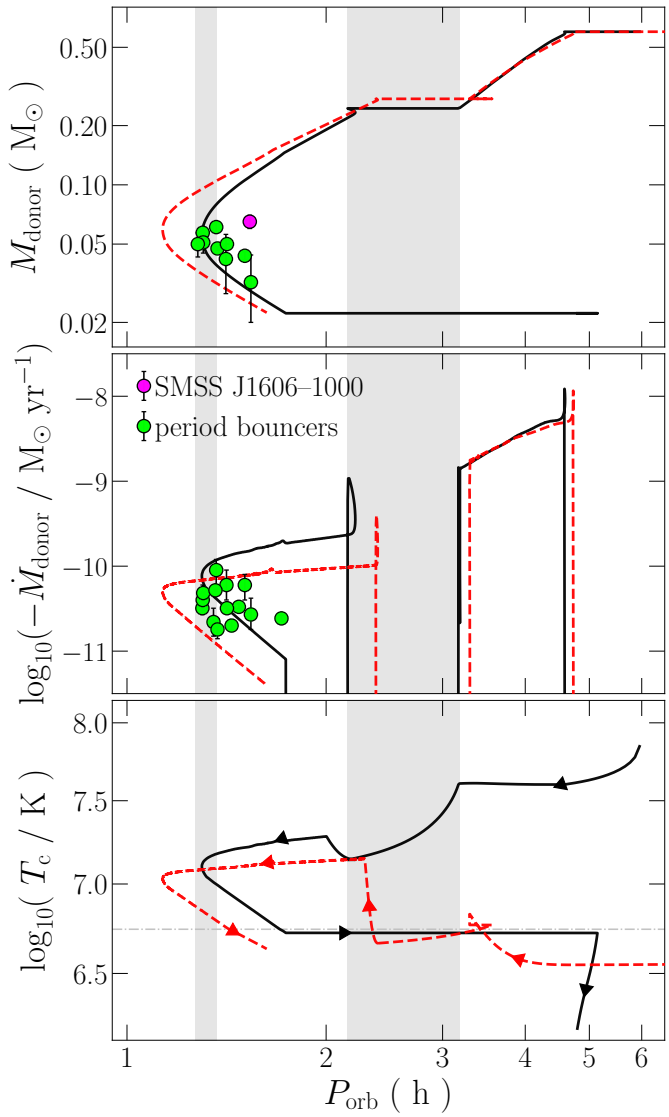

Fig. 1. Evolutionary tracks for two systems starting mass transfer above the gap. The initial parameters are $M_{\rm WD} = 0.8\,M_\odot$, $M_2 = 0.6\,M_\odot$, and $P_{\rm orb} = 0.25$ (black) and 1.0 days (red). The horizontal gray line in the bottom panel corresponds to $\log(Tc) = 6.742366$, which is the core temperature at the onset of crystallization. The vertical lines refer to the period minimum of $P_{\rm min} = 76-82$ min, and the period gap (2.15−3.18 h). While the system represented by the red track detaches above the gap because the white dwarf crystallizes before mass transfer starts, CVs that start mass transfer with a noncrystallizing white dwarf detach after they have passed the period minimum (black track). We note that the period minimum is at shorter periods for systems that previously generated a white dwarf magnetic field. This is because magnetic braking is reduced as some of the open field lines of the donor star are affected by the white dwarf magnetic field.

point. This causes the dynamo to generate a magnetic field which, after it has diffused to the white dwarf surface, connects with that of the donor and causes the secondary to detach from its Roche lobe.

The generated detached phase takes several Hubble times as the spin period has reached very small values because of the large amount of accreted angular momentum and because the remaining angular-momentum-loss mechanism is gravitational radiation (residual magnetic braking is suppressed through the connection of both magnetic fields; e.g. Belloni et al. 2020). The field strength needed to connect with the secondary star is much smaller than above the gap because the binary separation and mass-transfer rate are much smaller (see Schreiber et al. 2021, their Eq. (9)). As little as ∼1 MG is sufficient to generate a long detached phase.

In full analogy to what happens in the case where strong fields are generated in the 3–5 h orbital period range, the system appears first as a radio-pulsating fast-spinning white dwarf with a brown dwarf companion, before it synchronizes and becomes a pre-polar. Given that the spin angular momentum is typically high enough for the system to quickly evolve to periods of up to five hours, the age of the Galaxy is not sufficient for these detached systems to evolve back into a semi-detached configuration.

The tracks discussed above are representative of the majority of CVs, as most are born above the gap. If the core crystallizes before the onset of mass transfer, the magnetic field appears above or in the period gap. If, on the other hand, the white dwarf does not crystallize before the onset of mass transfer, it will only do so when the mass-transfer rate significantly drops after the system has passed the period minimum.

The situation is similar for CVs that start mass transfer in or below the gap. Figure 2 shows two tracks that describe the possible evolutionary pathways for such objects. The red dashed line corresponds to an evolution where the core of the white dwarf crystallizes before the onset of mass transfer, which causes the field to appear when the rotation criterion is met and the field has had time to diffuse to the white dwarf surface. This causes a relatively short (∼300 Myr) detached phase that occurs at a period similar to that of the onset of mass transfer (and before the period minimum is reached).

If the core does not crystallize before the onset of mass transfer (black line in Fig. 2), compressional heating of the white dwarf core during the mass transfer phase prevent crystallization until the mass accretion rate drops, which occurs after the binary has passed the period minimum. Compared to the case of CVs that started mass transfer above the gap with a noncrystallizing white dwarf, the maximum period reached during the detached phase is shorter because less angular momentum has been accreted, but it still takes longer than a Hubble time to evolve back to mass transfer.

While the exact evolution of a given system depends on the masses and orbital period of the detached post-common-envelope binary, virtually all CVs are predicted to evolve according to one of the four scenarios described above. The exceptions are CVs that become magnetic in the period gap. This might occur when the core of the white dwarf cools substantially before mass transfer but does not crystallize and accretion does not fully heat up the white dwarf core. To match all these conditions, some fine-tuning is required and therefore we expect relatively few systems to evolve in this way.

4. Predictions

Schreiber et al. (2021) invented the rotation- and crystallization-driven dynamo to explain the existence of detached post-common-envelope binaries with cool magnetic white dwarfs close to Roche-lobe filling in the period range of 3–5 h, the radio pulsing white dwarf binary AR Sco, and the fact that a large number of CVs contain a magnetic white dwarf. We here focus on the predictions of the model with respect to the evolution and magnetic field generation for CVs below the orbital period gap.

The relative number of CVs that are predicted to generate a magnetic field before the period minimum is reached, that is,

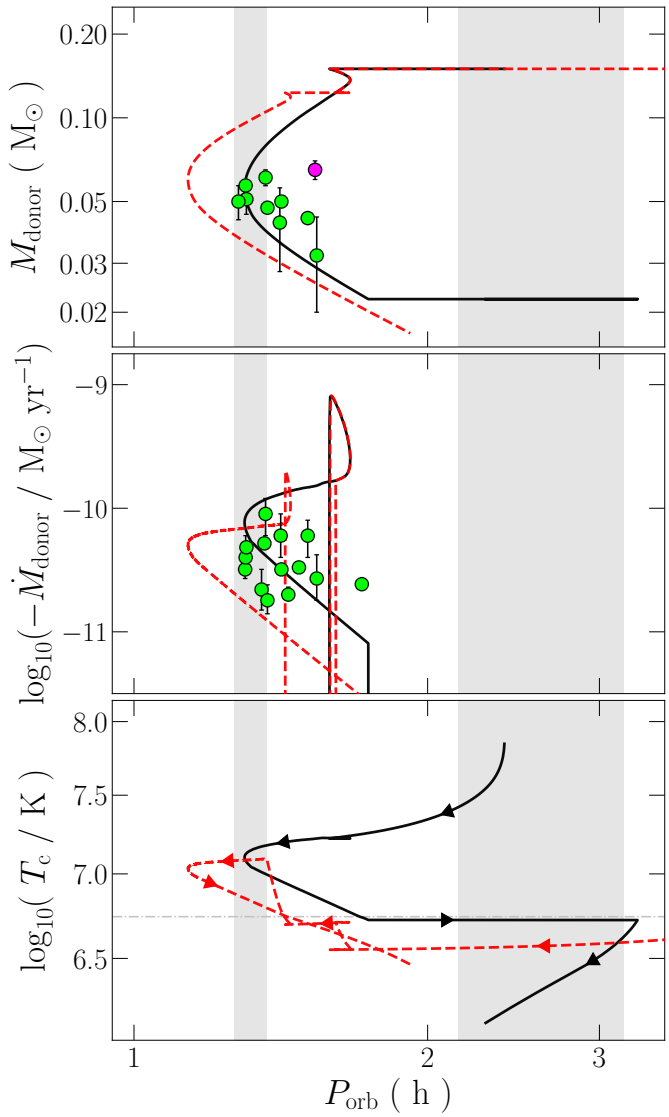

Fig. 2. Examples of evolutionary tracks for CVs starting mass transfer below the gap. The initial donor mass is assumed to be $M_2 = 0.15\,M_\odot$ and with initial post-common-envelope periods of 0.10 (black) and 0.25 days (red). If a CV is born with a crystallizing white dwarf, the magnetic field is generated before the period minimum is reached and the system detaches for a relatively short period of time (∼130 Myr) and then evolves as a magnetic CV through the period minimum (red dashed track). If the white dwarf does not start to crystallize before the onset of mass transfer, the binary detaches after it has passed the period minimum when the accretion rate became low enough to allow the white dwarf to crystallize (black solid track).

systems that either crystallize before mass transfer starts or in the period gap, depends on the initial mass-ratio distribution, common envelope efficiency, and the strengths of magnetic braking. Performing detailed binary population synthesis is beyond the scope of this Letter. However, assuming that a set of parameters for common envelope evolution, magnetic braking, and the initial mass ratio distribution exists that can explain the measured fraction of magnetic CVs, which is in the range of 20−40% (Pala et al. 2020; Inight et al. 2023a,b), it is straightforward to make testable predictions.

If the dynamo is fully responsible for magnetic field generation in CVs, ∼20−40% of all CVs either hosted a crystallizing white dwarf at the onset of mass transfer or the white dwarf crystallized in the period gap. These systems will pass the period minimum as magnetic CVs. The remaining ∼60−80% of all CVs evolve toward the period minimum as nonmagnetic CVs. Only after evolving through the period minimum can the core crystallize which causes the magnetic field to emerge and the binary to become a detached binary consisting of a magnetic white dwarf ($B \geq 1$ MG) with a brown dwarf companion. This reduces the fraction of expected period bouncers from 38−75% (Kolb 1993; Goliasch & Nelson 2015; Belloni et al. 2018) to ∼8−30% if we ignore the post-period-minimum evolution before the detached phase. This rough estimate represents an upper limit. If nonmagnetic CVs spend a significant time span as accreting CVs after having passed the period minimum and before the accretion rate sufficiently drops for the core to crystallize, the reduction of period bouncers might be significantly smaller than 60−80%. How long a given system spends as an accreting CV after having passed the period minimum depends on the crystallization temperature (which depends on the white dwarf mass) and the strength of angular momentum loss at this stage, which is not well known.

While detailed binary population synthesis is required to provide the exact numbers, we conclude that the dynamo, which was invented to explain the magnetic nature of CVs and detached systems with periods longer than 3 h, may bring the predicted relative numbers of period bouncers into agreement with the currently available observational constraints. The trade-off of this result is that the model predicts a large number of cool magnetic white dwarfs with brown dwarf companions, with a predicted space density similar to that of CVs with stellar companions. These systems might be difficult to detect because of the faintness of both stellar components and the absence of accretion. So far, there is only one known magnetic white dwarf that has a brown dwarf companion in a clearly detached binary that could be a detached CV (Kawka et al. 2021).

5. Conclusion

If a rotation- and crystallization-driven dynamo generates the magnetic field and the explanation for the existence of AR Sco and the detached magnetic white dwarf binaries in the orbital period range of 3−5 h presented by Schreiber et al. (2021) is correct, as a natural consequence, a large fraction of period bouncers must detach as soon as the accretion rate drops sufficiently and the white dwarf starts to crystallize. This may in principle explain the low number of period bouncers identified so far.

Even if the dynamo idea is found to be unfeasible, for example because the energy carried as kinetic energy in the convection zone is found to be insufficient to drive an efficient dynamo (Fuentes et al. 2023), the evolutionary scenario outlined in Schreiber et al. (2021) and in this Letter remains plausible as long as the magnetic field appearance in white dwarfs depends on their core temperature. There is indeed overwhelming evidence for the increased occurrence of magnetic fields in cool white dwarfs (Parsons et al. 2021; Bagnulo & Landstreet 2021).

Unequivocal proof for a temperature-dependent magnetic field generation in white dwarfs would be provided by the detection of a large number of detached binaries consisting of a cool ($\lesssim$10 000 K) magnetic ($\gtrsim$1 MG) white dwarf with a brown dwarf companion and orbital periods of between 80 min and a few hours. At present, just one such system is known (Kawka et al. 2021).

Acknowledgements. We are very grateful to the Kavli Institute for Theoretical Physics (KITP) for hosting the program "White Dwarfs as Probes of the Evolution of Planets, Stars, the Milky Way and the Expanding Universe". This research was supported in part by the National Science Foundation under Grant No. NSF PHY-1748958 and by the Munich Institute for Astro-, Particle and BioPhysics (MIAPbP) which is funded by the Deutsche Forschungsgemeinschaft (DFG, German Research Foundation) under Germany's Excellence Strategy – EXC-2094 – 390783311. MRS was supported from FONDECYT (grant number 1221059) and ANID, – Millennium Science Initiative Program – NCN19_171. DB acknowledges financial support from FONDECYT (grant number 3220167).

References

Amantayeva, A., Zharikov, S., Page, K. L., et al. 2021, ApJ, 918, 58
Angulo, C., Arnould, M., Rayet, M., et al. 1999, Nucl. Phys. A, 656, 3
Bagnulo, S., & Landstreet, J. D. 2021, MNRAS, 507, 5902
Bédard, A., Bergeron, P., Brassard, P., & Fontaine, G. 2020, ApJ, 901, 93
Belloni, D., & Schreiber, M. R. 2023, in Handbook of X-ray and Gamma-ray Astrophysics, eds. C. Bambi, & A. Santangelo, 129
Belloni, D., Schreiber, M. R., Zorotovic, M., et al. 2018, MNRAS, 478, 5626
Belloni, D., Schreiber, M. R., Pala, A. F., et al. 2020, MNRAS, 491, 5717
Belloni, D., Schreiber, M. R., Salaris, M., Maccarone, T. J., & Zorotovic, M. 2021, MNRAS, 505, L74
Buchler, J. R., & Yueh, W. R. 1976, ApJ, 210, 440
Cassisi, S., Potekhin, A. Y., Pietrinferni, A., Catelan, M., & Salaris, M. 2007, ApJ, 661, 1094
Chugunov, A. I., Dewitt, H. E., & Yakovlev, D. G. 2007, Phys. Rev. D, 76, 025028
Cyburt, R. H., Amthor, A. M., Ferguson, R., et al. 2010, ApJS, 189, 240
Epelstain, N., Yaron, O., Kovetz, A., & Prialnik, D. 2007, MNRAS, 374, 1449
Fuentes, J. R., Cumming, A., Castro-Tapia, M., & Anders, E. H. 2023, ApJ, 950, 73
Fuller, G. M., Fowler, W. A., & Newman, M. J. 1985, ApJ, 293, 1
Ginzburg, S., Fuller, J., & Kawka, A. 2022, MNRAS, 514, 4111
Goliasch, J., & Nelson, L. 2015, ApJ, 809, 80
Guidry, J. A., Vanderbosch, Z. P., Hermes, J. J., et al. 2021, ApJ, 912, 125
Hakala, P., Parsons, S. G., Marsh, T. R., et al. 2022, MNRAS, 513, 3858
Hurley, J. R., Tout, C. A., & Pols, O. R. 2002, MNRAS, 329, 897
Iglesias, C. A., & Rogers, F. J. 1993, ApJ, 412, 752
Iglesias, C. A., & Rogers, F. J. 1996, ApJ, 464, 943
Inight, K., Gänsicke, B. T., Breedt, E., et al. 2023a, MNRAS, 524, 4867
Inight, K., Gänsicke, B. T., Schwope, A., et al. 2023b, MNRAS, 525, 3597
Irwin, A. W. 2004, Astrophysics Source Code Library [record ascl:1211.002]
Isern, J., García-Berro, E., Külebi, B., & Lorén-Aguilar, P. 2017, ApJ, 836, L28
Itoh, N., Hayashi, H., Nishikawa, A., & Kohyama, Y. 1996, ApJS, 102, 411
Jermyn, A. S., Schwab, J., Bauer, E., Timmes, F. X., & Potekhin, A. Y. 2021, ApJ, 913, 72
Jermyn, A. S., Bauer, E. B., Schwab, J., et al. 2023, ApJS, 265, 15
Kawka, A., Vennes, S., Ferrario, L., et al. 2021, MNRAS, 507, L30
King, A. R., Regev, O., & Wynn, G. A. 1991, MNRAS, 251, 30P
Knigge, C., Baraffe, I., & Patterson, J. 2011, ApJS, 194, 28
Kolb, U. 1993, A&A, 271, 149
Langanke, K., & Martínez-Pinedo, G. 2000, Nucl. Phys. A, 673, 481
Littlefair, S. P., Dhillon, V. S., Marsh, T. R., et al. 2006, Science, 314, 1578
Littlefair, S. P., Dhillon, V. S., Marsh, T. R., et al. 2008, MNRAS, 388, 1582
Marsh, T. R., Gänsicke, B. T., Hümmerich, S., et al. 2016, Nature, 537, 374
McAllister, M. J., Littlefair, S. P., Dhillon, V. S., et al. 2017, MNRAS, 467, 1024
McAllister, M., Littlefair, S. P., Parsons, S. G., et al. 2019, MNRAS, 486, 5535
Muñoz-Giraldo, D., Stelzer, B., de Martino, D., & Schwope, A. 2023, A&A, 676, A7
Neustroev, V. V., & Mäntynen, I. 2023, MNRAS, 523, 6114
Neustroev, V. V., Marsh, T. R., Zharikov, S. V., et al. 2017, MNRAS, 467, 597
Oda, T., Hino, M., Muto, K., Takahara, M., & Sato, K. 1994, At. Data Nucl. Data Tables, 56, 231
Pala, A. F., Schmidtobreick, L., Tappert, C., Gänsicke, B. T., & Mehner, A. 2018, MNRAS, 481, 2523
Pala, A. F., Gänsicke, B. T., Breedt, E., et al. 2020, MNRAS, 494, 3799
Pala, A. F., Gänsicke, B. T., Belloni, D., et al. 2022, MNRAS, 510, 6110
Parsons, S. G., Gänsicke, B. T., Schreiber, M. R., et al. 2021, MNRAS, 502, 4305
Patterson, J. 2011, MNRAS, 411, 2695
Paxton, B., Bildsten, L., Dotter, A., et al. 2011, ApJS, 192, 3
Paxton, B., Cantiello, M., Arras, P., et al. 2013, ApJS, 208, 4
Paxton, B., Marchant, P., Schwab, J., et al. 2015, ApJS, 220, 15
Paxton, B., Schwab, J., Bauer, E. B., et al. 2018, ApJS, 234, 34
Paxton, B., Smolec, R., Schwab, J., et al. 2019, ApJS, 243, 10
Pelisoli, I., Marsh, T. R., Buckley, D. A. H., et al. 2023, Nat. Astron., 7, 931
Potekhin, A. Y., & Chabrier, G. 2010, Contrib. Plasma Phys., 50, 82
Rappaport, S., Verbunt, F., & Joss, P. C. 1983, ApJ, 275, 713
Rogers, F. J., & Nayfonov, A. 2002, ApJ, 576, 1064
Saumon, D., Chabrier, G., & van Horn, H. M. 1995, ApJS, 99, 713
Schreiber, M. R., Zorotovic, M., & Wijnen, T. P. G. 2016, MNRAS, 455, L16
Schreiber, M. R., Belloni, D., Gänsicke, B. T., Parsons, S. G., & Zorotovic, M. 2021, Nat. Astron., 5, 648
Schreiber, M. R., Belloni, D., Zorotovic, M., et al. 2022, MNRAS, 513, 3090
Timmes, F. X., & Swesty, F. D. 2000, ApJS, 126, 501
Townsley, D. M., & Bildsten, L. 2004, ApJ, 600, 390
Townsley, D. M., & Gänsicke, B. T. 2009, ApJ, 693, 1007
Unda-Sanzana, E., Marsh, T. R., Gänsicke, B. T., et al. 2008, MNRAS, 388, 889
van Spaandonk, L., Steeghs, D., Marsh, T. R., & Parsons, S. G. 2010, ApJ, 715, L109
Webbink, R. F., & Wickramasinghe, D. T. 2002, MNRAS, 335, 1
Zharikov, S. V., Tovmassian, G. H., Neustroev, V. V., et al. 2008, A&A, 486, 505
Zorotovic, M., Schreiber, M. R., & Gänsicke, B. T. 2011, A&A, 536, A42

Appendix A: Modeling details

The equations describing most of the ingredients of the model, such as the white dwarf spin-up and orbital angular momentum loss, are given in Schreiber et al. (2021). We report all parameters and revised assumptions below.

A.1. MESA

We used the MESA code (Paxton et al. 2011, 2013, 2015, 2018, 2019; Jermyn et al. 2023, r15140) to compute the evolution of CVs and their progenitors. The MESA equation of state is a blend of the OPAL (Rogers & Nayfonov 2002), SCVH (Saumon et al. 1995), FreeEOS (Irwin 2004), HELM (Timmes & Swesty 2000), PC (Potekhin & Chabrier 2010) and Skye (Jermyn et al. 2021) equations of state. Nuclear reaction rates are a combination of rates from NACRE (Angulo et al. 1999), JINA REACLIB (Cyburt et al. 2010), plus additional tabulated weak reaction rates (Fuller et al. 1985; Oda et al. 1994; Langanke & Martínez-Pinedo 2000). Screening is included via the prescription of Chugunov et al. (2007) and thermal neutrino loss rates are from Itoh et al. (1996). Electron conduction opacities are from Cassisi et al. (2007) and radiative opacities are primarily from OPAL (Iglesias & Rogers 1993, 1996), with the high-temperature Compton-scattering-dominated regime calculated using the equations of Buchler & Yueh (1976).

A.2. Spin-up of the white dwarf

The spin up of accreting white dwarfs was calculated as in Schreiber et al. (2021, their eq. 1) assuming an initial spin period of one year and the maximum spin-up efficiency of $\alpha = 1$. The angular momentum loss parameter of the white dwarf due to nova explosions was set to $\eta = 0.833$ which corresponds to a slightly nonspherical ejection. The critical spin period for the generation of a magnetic field was set to one hour. We assumed the white dwarf mass to be constant during CV-evolution, that is, we assume the accreted mass to be ejected during nova eruptions.

A.3. Orbital angular momentum loss

For secondary stars with a radiative core and convective envelope, we assumed angular momentum loss through magnetic braking according to Rappaport et al. (1983, with $\gamma = 3$) with a normalization factor of 0.6 (Knigge et al. 2011). In case the magnetic field of the white dwarf connects with that of the secondary star, we assumed that magnetic braking is reduced as described in Webbink & Wickramasinghe (2002) and Belloni et al. (2020).

Angular momentum loss through gravitational radiation was calculated using the weak-field approximation of general relativity as in Hurley et al. (2002). We assumed residual magnetic braking for fully convective donor stars and approximated it by multiplying angular momentum loss through gravitational radiation by 1.5 which provides accretion rates below the gap in agreement with the observations (Knigge et al. 2011). We assumed the empirical consequential angular momentum loss prescription of Schreiber et al. (2016, their eq. 5) with a normalization factor of $C = 0.35$.

A.4. Cooling and heating of the white dwarf

We follow the cooling of nonaccreting white dwarfs using the models by Bédard et al. (2020). Incorporating the full details of cooling and heating of accreting white dwarfs in our simulations is beyond the scope of this paper. We instead incorporated a simple prescription based on published results (Townsley & Bildsten 2004; Epelstain et al. 2007; Townsley & Gänsicke 2009).

In cases where the cooling temperature of the white dwarf at the onset of mass transfer is below the temperature generated by compressional heating (Townsley & Gänsicke 2009, their equation 1), the white dwarf core temperature is heated on timescales of a few hundred million years until the equilibrium luminosity $L_{\rm eq} \simeq \langle \dot{M} \rangle T_{\rm c}/\mu m_{\rm p} = 4\pi R^2 \sigma T_{\rm eff}^4$ is reached. Here, $T_{\rm c}$ is the core temperature assumed to be equal to that at the base of the radiative layers, R is the white dwarf radius, μ is the mean molecular weight of the accreted material, $m_{\rm p}$ is the mass of the proton, and σ is the Stefan–Boltzmann constant (see Townsley & Gänsicke 2009, for more details).

Throughout this work we assume that the timescale required to reach the equilibrium temperature is 200 Myr. When mass transfer starts and the compressional heating temperature exceeds the cooling temperature of the white dwarf, we slowly increase the core temperature interpolating between the cooling temperature and the equilibrium temperature using a cubic equation. The latter makes sure that the increase in temperature is slow at the beginning (Epelstain et al. 2007). If mass transfer stops, the white dwarf temperature is assumed to follow again the cooling models from Bédard et al. (2020) but starting from the core temperature reached during accretion.

In the case where the cooling temperature of the white dwarf is hotter than the temperature derived from compressional heating, the cooling temperature of course should represent the true white dwarf core temperature. In this case, we therefore assume the usual cooling of a nonaccreting white dwarf to determine the timescale on which the equilibrium between compressional heating and core temperature is reached.

A.5. Dynamo conditions and synchronization

We assumed the generation of a magnetic field to require the core temperature of the white dwarf to have reached the onset of crystallization according to the cooling models by Bédard et al. (2020) and a spin period shorter than one hour. Once the conditions for the dynamo to work are met, we assume a delay for the appearance of the magnetic field on the surface of the white dwarf. This timescale depends on the mass and the temperature of the white dwarf (Ginzburg et al. 2022, their fig. 3). Here, we only show tracks for white dwarfs of the canonical mass for white dwarfs in CVs (0.8 $M_\odot$, Zorotovic et al. 2011) and assume a diffusion timescale of 10^8 yr.

We assumed a magnetic field of 1 kG for the donor star independent of its mass and the generated white dwarf magnetic field to be of 60 MG. The synchronization timescale as defined in Schreiber et al. (2021) was set to 1 Myr.

A.6. Other parameters

We assumed a maximum evolutionary time of 10 Gyr. We start all our simulations with a detached post-common-envelope binary assuming that the formation of the white dwarf takes 300 Myr. We calculated the evolution for a white dwarf mass of 0.8 $M_\odot$ and donor masses of 0.15 and 0.6 $M_\odot$. The initial orbital periods of the post common envelope binary were assumed to be between 0.1 − 1 days.

Appendix B: Observed period bouncers

In order to be able to compare our evolutionary tracks with observed systems, we compiled a list of observed period bouncers (Table B.1). We only included systems with measured orbital period as well as donor mass and/or accretion rate.

Three out of 20 systems contain a magnetic white dwarf which corresponds to a fraction of 15 ± 7 per cent in rough agreement with the number of magnetic CVs in the SDSS sample (Inight et al. 2023a,b) but smaller than in the volume limited 150 pc sample (Pala et al. 2020).

We found one system that could perhaps be a detached magnetic CV: SMSSJ 160639.78−100010.7 consists of a magnetic white dwarf with a brown dwarf companion orbiting their common center of mass in 92 minutes (Kawka et al. 2021). While for the measured white dwarf mass, the temperature seems to be slightly too hot for the white dwarf to be crystallizing, the system could be explained by a CV with a white dwarf that crystallized before the onset of mass transfer. In this scenario, the mass transfer must have started below the gap with a low-mass M-dwarf companion ($\lesssim 0.1\,M_\odot$). Two promising candidate detached magnetic period bouncers are ZTF J014635.73+491443.1 and SDSS J121209.31+013627.7 (Hakala et al. 2022; Guidry et al. 2021). We do not list these candidates in Table B.1 because of uncertainties related to the measured period or the nature of the donor star. Interestingly, ZTF J014635.73+491443.1 is nearby (56 pc), which might indicate that such systems are not rare.

Table B.1. Properties of confirmed and candidate period bouncers.

System	$P_{\rm orb}$ (min)	$\langle \dot{M}_{\rm d} \rangle$ ($10^{-10}\,M_\odot\,{\rm yr}^{-1}$)	$M_{\rm d}$ ($M_\odot$)	ref.
SDSS J143544.02+233638.7	78.00	$0.32^{+0.08}_{-0.05}$		1, 2
SDSS J143317.78+101123.3	78.10	$0.40^{+0.20}_{-0.10}$	0.0571 ± 0.001	1, 2
V455 And	81.08	$0.22^{+0.10}_{-0.07}$		1, 2
SDSS J150137.22+550123.3	81.85	0.90 ± 0.30	0.061 ± 0.004	1, 2
SDSS J103533.02+055158.4	82.22	$0.18^{+0.06}_{-0.04}$	0.0475 ± 0.001	3, 2
SDSS J150240.98+333423.9	84.83	$0.6^{+0.3}_{-0.2}$		4
EG Cnc	86.36	$0.2^{+0.03}_{-0.02}$		4
1RXS J105010.8−140431	88.56	$0.332^{+0.028}_{-0.018}$		4
QZ Lib	92.36	$0.27^{+0.15}_{-0.09}$	0.032 ± 0.012	4
GD 552	102.73	$0.243^{+0.023}_{-0.018}$		5, 6
BW Scl	78.23	$0.483^{+0.014}_{-0.012}$	0.051 ± 0.006	7, 6
WZ Sge	81.63	$0.52^{+0.014}_{-0.01}$		8, 6
SDSS J080434.20+510349.2	84.97	0.32 ± 0.03		8, 6
SDSS J105754.25+275947.5	90.42	0.60 ± 0.20	0.0436 ± 0.0020	9
GW Lib	76.78		0.050 ± 0.007	10
EZ Lyn	84.66		0.042 ± 0.014	11
CRTS J122221.6−311525	109.80		0.036 ± 0.010	12
SDSS J125044.42+154957.4[a]	86.30	1.7×10^{-4}		13
V379 Vir[a]	88.40	5.3×10^{-4}		13
SDSSJ 151415.65+074446.5[a]	88.70	5.9×10^{-4}		13
SMSSJ 160639.78−100010.7[a]	92.00		0.065 ± 0.005	14

Notes. [(a)] Magnetic systems that are presumably period bouncers and the detached magnetic white dwarf plus brown dwarf binary SMSSJ 160639.78−100010.7 which might be a detached CV.

References. (1) Littlefair et al. (2008) (2) McAllister et al. (2019); (3) Littlefair et al. (2006); (4) Pala et al. (2018); (5) Unda-Sanzana et al. (2008); (6) Pala et al. (2022); (7) Neustroev & Mäntynen (2023); (8) Zharikov et al. (2008); (9) McAllister et al. (2017); van Spaandonk et al. (2010); (11) Amantayeva et al. (2021); (12) Neustroev et al. (2017); (13) Muñoz-Giraldo et al. (2023); (14) Kawka et al. (2021)